# Photonic Aharonov-Bohm Effect Based on Dynamic Modulation

Kejie Fang
*Department of Physics, Stanford University, Stanford, California 94305, USA*

Zongfu Yu and Shanhui Fan
*Department of Electrical Engineering, Stanford University, Stanford, California 94305, USA*

(Received 19 October 2011; published 12 April 2012)

We show that when the refractive index of a photonic system is harmonically modulated, the phase of the modulation introduces an effective gauge potential for photons. This effective gauge potential can be used to create a photonic Aharonov-Bohm effect. We show that the photonic Aharonov-Bohm effect provides the optimal mechanism for achieving complete on-chip nonmagnetic optical isolation.

DOI: 10.1103/PhysRevLett.108.153901 PACS numbers: 42.82.Et, 03.65.Vf, 42.79.Nv

The Aharonov-Bohm effect [1] is a very important effect in quantum physics, since it demonstrates the importance of the gauge potential for electrons. It is of fundamental interest to ask whether an analogous Aharonov-Bohm effect can be created for photons. The answer to this question has proved elusive: Photons are neutral particles, and therefore there is no natural gauge potential that couples to a photon. In this Letter, we exploit the concept of photonic transition as induced by the dynamic modulation of a material's permittivity [2–4] and show that the *phase* of the modulation can be used to create an effective gauge potential and, hence, a photonic Aharonov-Bohm effect. As an application, we show that such a photonic Aharonov-Bohm effect leads to the design of an on-chip nonmagnetic photonic isolator that is significantly simpler compared with the currently available designs.

To start, we first briefly review the concept of photonic transition [2–5]. We consider a slab waveguide where light propagates along the $z$ direction [Fig. 1(a)]. The waveguide supports two photonic bands of transverse electric modes (electric field along the $y$ direction) with even and odd symmetry with respect to the center of the waveguide [Figs. 1(b) and 1(c)]. Here, for simplicity, we have considered only a two-dimensional system. However, our design should be applicable to three-dimensional waveguides, as has been demonstrated in three-dimensional numerical simulations and experiments [6]. We consider an even mode $|1\rangle$ and an odd mode $|2\rangle$, with frequencies $\omega_1$ and $\omega_2$ and with the same wave vector $k$. A photonic transition between $|1\rangle$ and $|2\rangle$ can be induced with a dielectric modulation:

$$\epsilon(t) = \epsilon_s + \delta(x)\cos(\Omega t + \phi), \tag{1}$$

where $\Omega = \omega_2 - \omega_1$. The transition takes place as the photons propagate along the waveguide under modulation. Note that the modulation here as described by a profile $\delta(x)$ is uniform along the $z$ direction. Hence, the wave vector of the modes is conserved in the photonic transition, and thus the transition is direct. This is in contrast with Refs. [4,5], where the modulation was of a traveling wave form that induced an indirect transition.

The electric field in the modulated waveguide can be expressed as [4]

$$E_k(x, z, t) = a_1(z)E_{1k}(x)e^{i(-kz+\omega_1 t)} + a_2(z)E_{2k}(x)e^{i(-kz+\omega_2 t)}, \tag{2}$$

where $k$ is the wave vector along the $z$ direction and $E_{1k,2k}(x)$ are the modal profiles of the even and odd modes, respectively, normalized such that $|a_n|^2$ is the photon

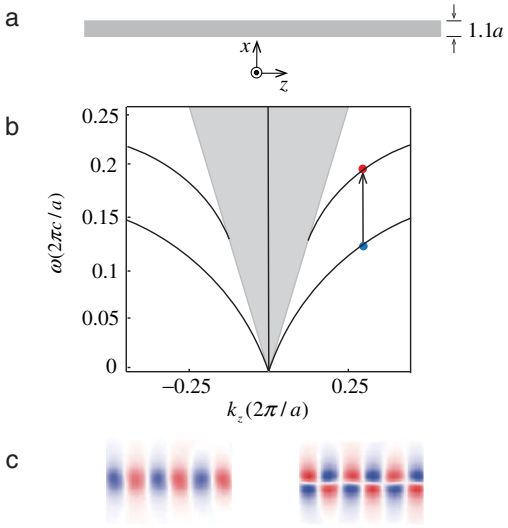


FIG. 1 (color online). (a) A silicon slab waveguide. The width of the waveguide is $1.1a$. The $x$-$z$ plane is parallel to the surface of the waveguide. We consider only two-dimensional propagation in the $x$-$z$ plane. (b) Band structure of the waveguide. The first and second bands are the fundamental even and odd transverse electric modes, respectively, both having an electric field only along the $y$ direction. The gray area is the light cone. The photonic transition is induced vertically between an even mode (blue dot) and an odd mode (red dot). (c) Modal profile of the even mode (left) and the odd mode (right).

 

number flux carried by the $n$th mode [7]. Equation (2) assumes that the modulation is weak as compared to the dielectric constant of the structure and that the modulation can provide phase-matched coupling only between these two states. Substituting Eq. (2) into Maxwell's equation, we obtain the coupled mode equation [8]

$$i\frac{d}{dz}\begin{pmatrix} a_1 \\ a_2 \end{pmatrix} = \begin{pmatrix} 0 & Ce^{-i\phi} \\ C^{\star}e^{i\phi} & 0 \end{pmatrix}\begin{pmatrix} a_1 \\ a_2 \end{pmatrix}, \tag{3}$$

where $C = -\frac{1}{8}\int \delta(x)E_{1k}^{\star}(x)E_{2k}(x)dx$. In order to have $C \neq 0$, for the two modes considered here that have opposite symmetry, $\delta(x)$ cannot be uniform along the $x$ direction. The solution of this coupled mode equation can be expressed by a transfer matrix $T(\phi)$, relating the mode amplitudes $a_n'(z) = a_n(z)e^{-ikz}$ at the positions of $z$ and 0:

$$\begin{pmatrix} a_1'(z) \\ a_2'(z) \end{pmatrix} = T(\phi)\begin{pmatrix} a_1'(0) \\ a_2'(0) \end{pmatrix}, \tag{4}$$

$$T(\phi) = e^{-ikz}\begin{pmatrix} \cos(Cz) & ie^{-i\phi}\sin(Cz) \\ ie^{i\phi}\sin(Cz) & \cos(Cz) \end{pmatrix}. \tag{5}$$

The coupled mode equation of the waveguide system [Eq. (3)] corresponds to a Hamiltonian $H = Ce^{-i\phi}a_1^{\dagger}a_2 + Ce^{i\phi}a_2^{\dagger}a_1$ (if we do a substitution of $z = vt$ and set $v = 1$, where $v$ is the group velocity of the waveguide mode). The phase $\phi$ thus describes a gauge transformation of the system [9]. There is an arbitrariness in choosing $\phi$, since as we see in Eq. (1) it is related to the time origin of the modulation, which can be arbitrarily set. Also, in association with this phase, one can construct a gauge potential in analogy to a lattice model for an electron. Consider an electronic lattice model described by a tight-binding Hamiltonian $H = \sum_{r',r} C_{r',r}^0 b_{r'}^{\dagger} b_r$ in the absence of a magnetic field, where $C_{r',r}^0$ is the hopping coefficient between states $b_r$ and $b_{r'}$. In the presence of a magnetic field, as described by a gauge potential $\vec{A}(\vec{r})$, the Hamiltonian is modified via the Peierls substitution [10] to $H' = \sum_{r',r} C_{r',r} b_{r'}^{\dagger} b_r$, where $C_{r',r} = e^{i(e/\hbar)\int_r^{r'} \vec{A}\cdot d\vec{l}} C_{r',r}^0 \equiv e^{i\phi} C_{r',r}^0$. Thus, the phase $\phi$ in the coupling constant $C_{r',r}$ is associated with a gauge potential through

$$\frac{e}{\hbar}\int_r^{r'} \vec{A}\cdot d\vec{l} = \phi. \tag{6}$$

Similarly, for the photonic system considered here, we can associate a gauge potential $\vec{A}$ to the phase $\phi$ through $\int_1^2 \vec{A}\cdot d\vec{l} = \phi$, where 1 and 2 represent the spatial locations of the two photonic states $|1\rangle$ and $|2\rangle$, respectively (the spatial location of a state can be defined as the center of mass of the photon field distribution). In the special case, where the two states are colocated spatially, $\vec{A}$ is singular. Nevertheless, the line integral of $\vec{A}$ in Eq. (6), which is the only relevant physical quantity for a gauge potential [11], is finite. Also, since the line integral depends on the direction of integration, we have $\int_2^1 \vec{A}\cdot d\vec{l} = -\phi$. Thus, while a photon does not carry any charge, we nevertheless find that the phase of the dynamic modulation can create a gauge potential for photons.

In this system, all operations on the photon modes belong to a $SU(2)$ group. However, the gauge transformation here is connected to the arbitrariness in setting a single relative phase factor between the components of states $|1\rangle$ and $|2\rangle$. Since there is only a single such phase factor, the corresponding gauge degree of freedom has a $U(1)$ symmetry. This is fundamentally different from the $SU(2)$ gauge field as described in Ref. [12], where the gauge degrees of freedom themselves have a $SU(2)$ symmetry.

One of the most prominent consequences of a gauge potential is the Aharonov-Bohm effect. For electrons, the typical geometry for demonstrating this effect is shown in Fig. 2, where two arms of electron waveguides are connected on either end at $z_1$ and $z_2$ by a waveguide coupler, to form a ring enclosing a magnetic flux. We denote the states that correspond to an electron in either of the two waveguides as $|1\rangle$ and $|2\rangle$, respectively. Imagine that one injects an electron into waveguide 1 from the left and measures the transmission amplitude in waveguide 1 on the right [Fig. 2(a)]. There are two separate pathways that contribute to such a transmission amplitude. The first pathway consists of an electron emerging from the first coupler as state $|2\rangle$, propagating along the upper arm, and then going through the second coupler returning to state $|1\rangle$. In the second pathway, the electron remains in state $|1\rangle$ as it passes through the two waveguide couplers. The phase difference between these two pathways is then

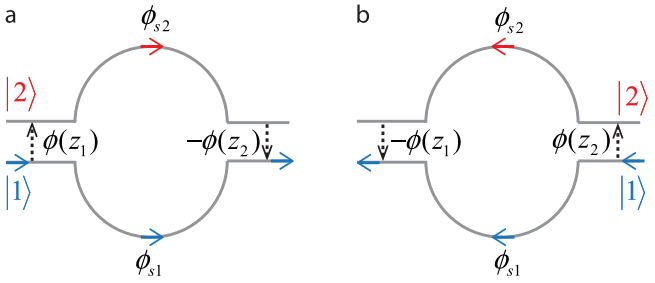


FIG. 2 (color online). Illustration of the Aharonov-Bohm effect for both an electron and a photon, with the particle injected from (a) the left or (b) the right of the structure. In the case of the electron, the structure consists of two waveguides coupled together through two waveguide couplers at the end, forming a ring that encloses a magnetic flux. The dashed arrows correspond to the location of the waveguide couplers. $|1\rangle$ and $|2\rangle$ represent the quantum states of having the electron in either waveguide. In the case of the photon, this plot is used to illustrate the interference effect for the structure in Fig. 3(a). Here $|1\rangle$ and $|2\rangle$ represent the even and odd modes in the waveguides, respectively. The dashed arrows represent photonic transition as induced by dynamic modulation.

$$\phi_{s2} - \phi_{s1} + \pi + \frac{e}{\hbar}\oint \vec{A}\cdot d\vec{l}, \tag{7}$$

where $\phi_{s2} - \phi_{s1} + \pi$ describes the accumulated phase difference between the two pathways in the absence of the magnetic field, with $\phi_{s1}$ and $\phi_{s2}$ being the accumulated propagation phases in the two arms, the extra phase $\pi$ arising due to the beam splitter. $\oint \vec{A}\cdot d\vec{l}$ describes the effect of the magnetic field. The physics of a gauge potential in general depends only on such a line integral $\oint \vec{A}\cdot d\vec{l}$ on a closed path. Therefore, we are free to choose a gauge such that $\int \vec{A}\cdot d\vec{l}$ is nonvanishing only at the waveguide couplers, in which case

$$\frac{e}{\hbar}\oint \vec{A}\cdot d\vec{l} = \frac{e}{\hbar}\int_1^2 \vec{A}(z_1)\cdot d\vec{l} - \frac{e}{\hbar}\int_1^2 \vec{A}(z_2)\cdot d\vec{l} \equiv \phi(z_1) - \phi(z_2). \tag{8}$$

Based on the description of the Aharonov-Bohm effect above, we create an analogous photonic Aharonov-Bohm effect using dynamic modulation, in a structure as shown in Fig. 3(a). The structure consists of two modulated waveguide regions, centered at $z_1$ and $z_2$, each modulated with a modulation phase $\phi(z_1)$ and $\phi(z_2)$, respectively. Between the two modulated waveguide regions is a central waveguide region that is unmodulated and, in general, can have a width different from the modulated waveguide. The even and odd modes, upon passing through the central waveguide, acquire different phases $\phi_{s1}$ and $\phi_{s2}$, respectively. The corresponding transfer matrix is

$$T_f = \begin{pmatrix} e^{i\phi_{s1}} & 0 \\ 0 & e^{i\phi_{s2}} \end{pmatrix}. \tag{9}$$

The interference process for the structure in Fig. 3(a) can also be illustrated with Fig. 2, provided that we now associate states $|1\rangle$ and $|2\rangle$ with the even and odd modes in the photonic waveguide instead. Compared with the electronic Aharonov-Bohm effect, the two waveguide couplers are now replaced by the two modulated waveguide regions, whereas the central waveguide region plays the role of the arms. Suppose that we inject a photon in the even mode $|1\rangle$ from the left and measure the transmitted amplitude in the even mode $|1\rangle$ at the right [Fig. 2(a)]. The transmitted amplitude again results from the interference of two pathways. In the first pathway, the photon state undergoes an upward transition at $z_1$, propagates as the odd mode $|2\rangle$, and then undergoes a downward transition at $z_2$, acquiring a phase $\phi_{s2} + \pi + \phi(z_1) - \phi(z_2)$ (note that the extra $\pi$ phase comes from the $i$ factor in the off-diagonal components of the transfer matrix [Eq. (5)]). In the second pathway, the photon state does not undergo any transitions and acquires a phase $\phi_{s1}$ as it propagates as the even mode $|1\rangle$. The phase difference between the two pathways is then $\phi_{s2} - \phi_{s1} + \pi + \phi(z_1) - \phi(z_2)$. Comparing this phase with Eqs. (7) and (8) for the electronic case, we see that the phases $\phi(z_1)$ and $\phi(z_2)$ due to dynamic modulation play exactly the same role as the magnetic-field-dependent phase in the electronic Aharonov-Bohm effect. This discussion of the Aharonov-Bohm effect based on a line integral of the gauge potential is equivalent to the discussion based on the Berry phase [13]. In particular, the phase factor $\phi(z_1) - \phi(z_2)$ is the Berry phase as a photon goes through a round trip in this structure.

Although either $\phi(z_1)$ or $\phi(z_2)$ is arbitrary, since it depends on the choice of the time origin, $\phi(z_1) - \phi(z_2)$ is fixed, since a time translation $t \rightarrow t + \Delta t$ would change

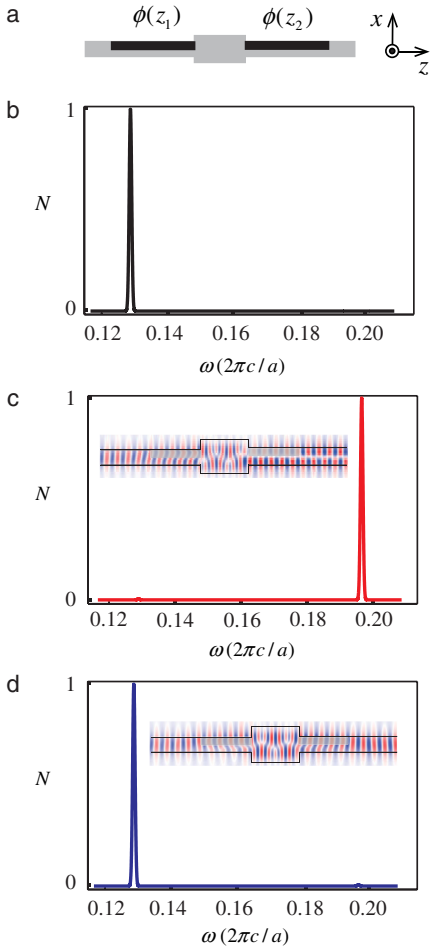


FIG. 3 (color online). (a) Waveguide isolator structure ($x$-$z$ plane) simulated by using the finite-difference time-domain method (the length along the $z$ direction is compressed by a factor of $1/4$). The width of the modulated waveguide is $1.1a$, and the width of the central waveguide region is $2.0a$. The modulation covers only the upper half of the waveguide (black region). The length of a single modulated region and the central waveguide region is $19a$ and $11.6a$, respectively. The phase of the modulation on the left and right is 0 and $\pi/2$, respectively. (b) Incident photon flux. (c),(d) Transmitted photon flux through the structure in (a) when the pulse of (b) is incident from the left (c) and right (d), respectively. The insets are the distribution of the electric field (the length along the $z$ direction is compressed by a factor of $1/4$), and the gray regions are the modulated regions.

$\phi(z_1)$ and $\phi(z_2)$ by the same value $\Omega\Delta t$. This means that the phase difference of the two pathways is gauge-independent, just like the magnetic-field-dependent phase $\frac{e}{\hbar}\oint\vec{A}\cdot d\vec{l}$ in the electronic Aharonov-Bohm effect.

In the electronic Aharonov-Bohm effect, the time-reversal symmetry is broken. When an electron is instead injected from the right end of waveguide 1, and we consider the transmission amplitude in waveguide 1 at the left end [Fig. 2(b)], the phase difference of the two pathways is $\phi_{s2}-\phi_{s1}+\pi-\frac{e}{\hbar}\oint\vec{A}\cdot d\vec{l}=\phi_{s2}-\phi_{s1}+\pi-\phi(z_1)+\phi(z_2)$, where the magnetic-field-dependent phase flips sign. Similarly, the photonic system also has broken time-reversal symmetry. The dynamical modulation $V\cos(\Omega t+\phi)$ is not invariant under a time-reversal operation $t\rightarrow -t$, if $\phi\neq 0$. Thus, the time-reversal symmetry breaking for a single modulated region is gauge-dependent and does not have a real physical effect. On the other hand, in our photonic Aharonov-Bohm interferometer, with the two waveguide regions modulated with different phases, at least one of the modulated regions must have a nonzero modulation phase. Consequently, the time-reversal symmetry breaking becomes gauge-independent and therefore physical. As a result, if we inject a photon state $|1\rangle$ in the second modulated waveguide [Fig. 2(b)], as the state propagates to the first modulated waveguide, the phase difference of the two pathways is $\phi_{s2}-\phi_{s1}+\pi-\phi(z_1)+\phi(z_2)$, where the modulation-induced phase flips sign, since, as can be seen from Eq. (3), upward and downward transitions acquire opposite phases.

One application of such a photonic Aharonov-Bohm effect is to achieve nonmagnetic optical isolation. By choosing the modulation phases satisfying $\phi(z_2)-\phi(z_1)=\pi/2$, the length $L$ of the modulated region to be $\pi/(4C)$, and the length of the central waveguide region such that $\phi_{s2}-\phi_{s1}=\pi/2$, we have the transfer matrix for modes propagating to the right:

$$T_r=T(\phi_2)T_fT(\phi_1)=e^{-i(2kL-\phi_{s1})}\begin{pmatrix}0 & i\\ -1 & 0\end{pmatrix}. \quad (10)$$

With the same modulation, for modes propagating to the left, the total transfer matrix becomes

$$T_l=T(\phi_1)T_fT(\phi_2)=e^{-i(2kL-\phi_{s1})}\begin{pmatrix}1 & 0\\ 0 & i\end{pmatrix}. \quad (11)$$

Thus, an even mode injected at $\omega_1$ from the left is completely converted to an odd mode after passing through the structure. An even mode injected from the right, however, stays an even mode after passing through the structure. In this case, therefore, we have used the photonic Aharonov-Bohm effect to create an optical isolator.

Optical isolators are traditionally based on the magneto-optical effect [14–18], which is incompatible with on-chip integration. Isolation based on dynamical modulation can overcome this material difficulty [4,19,20]. References [4,19,20] rely upon a traveling wave modulation profile. Such a modulation profile can be implemented by separately modulating a large number of regions, with each region being modulated uniformly but different regions having different modulation phases. In contrast to Ref. [4], the scheme proposed in this Letter uses only two uniformly modulated regions with different modulation phases. Since as argued above, in a modulated system, time-reversal symmetry breaking is gauge-independent only if we use at least two regions modulated at different phases, we have here proposed the optimal dynamic optical isolator design in terms of the number of regions that need to be modulated.

We demonstrate the interference effect and the isolator concept as discussed above by using finite-difference time-domain simulations. The waveguide is made of silicon with $\epsilon_s=12.25$. The two modulated regions have a width of $1.1a$, where $a$ is a length unit [Fig. 3(a)]. The direct interband transition is induced between an even mode with a frequency $\omega_1=0.129(2\pi c/a)$ and an odd mode with a frequency $\omega_2=0.197(2\pi c/a)$, by a permittivity modulation $\delta\epsilon(t)=0.1\epsilon_s\cos(\Omega t+\phi)$, where $\Omega=\omega_2-\omega_1$. We set the phase of the modulation to be 0 and $\pi/2$ for the modulated regions on the left and right, respectively. To maximize the transition between the even and odd modes, the modulated region covers only the upper half of the waveguide in the $x$ direction [4]. The length of each modulated region is $19a$. The central waveguide region has a width of $2a$ and a length of $11.6a$, such that the even and odd modes, upon passing through this region, acquire a $\pi/2$ phase difference. The finite-difference time-domain simulation result is shown in Fig. 3. It agrees with the transfer matrix analysis, as complete transition from an even mode to an odd mode occurs for one direction, while no transition happens for the opposite direction, with a contrast ratio above 25 dB.

The state-of-the-art silicon modulators can achieve a modulation frequency of 20 GHz and an index modulation strength of $\delta/\epsilon_s=5\times 10^{-4}$ [21,22]. Within such a practical constraint, and using the coupled mode theory above, we design the structure as shown in Fig. 4. Each of the two modulated regions now consists of two single-mode waveguides brought in close proximity to each other. The width of each waveguide is 0.20 $\mu$m. The air gap between them has a width of 0.76 $\mu$m. These parameters are chosen such that the two waveguides couple to each other to form a pair of even and odd eigenmodes that have a frequency difference of 20 GHz. Only one of the two waveguides is modulated. The length of the modulated region is

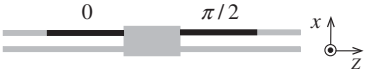


FIG. 4. The structure for experimental realization of the photonic Aharonov-Bohm effect. The gray regions are dielectric waveguides. The two black regions are modulated, with modulation phases of 0 and $\pi/2$, respectively.

4.36 mm. The center waveguide region, which is unmodulated, has a width of 2 $\mu$m and a length of 6.90 $\mu$m. The resulting simulation using coupled mode theory indicates that the structure functions as an isolator, with a contrast ratio exceeding 25 dB, over a bandwidth of 1.25 THz. In a modulated waveguide, propagation loss due to the carrier injection is typically the dominant loss mechanism. The free carrier loss for a modulation strength of $\delta/\epsilon_s = 5 \times 10^{-4}$ is about 1.5 $\mathrm{cm}^{-1}$ [23]. Thus, the propagation of light over a distance of millimeters, as required for our isolator device, is quite achievable. Moreover, since such a loss applies to transmission in both directions, the isolation contrast ratio remains the same in the presence of such a loss. In aiming to achieve a large bandwidth, the even and odd modes need to have parallel bands [4,5], i.e., having matching group velocity. When such parallel bands are achieved, the bandwidth is then limited by the higher-order dispersions of the waveguide modes. Since such a bandwidth is far smaller than the optical frequency, the variation of the modal profile within the bandwidth, which would have resulted in the variation of coherence length as a function of frequency, is negligible [4,5].

In conclusion, we show that, in a dynamically modulated photonic system, the phase of the modulation can be used to create an effective gauge potential for photon states. This concept can be applied to induce a photonic Aharonov-Bohm effect. As an application, we show that the use of such a gauge potential concept can greatly simplify dynamic isolator design. More generally, we anticipate that such an effective gauge potential can generate many other novel phenomena in photonic systems that are analogous to a charged system coupled to a magnetic field.

This work is supported in part by U.S. Air Force Office of Scientific Research Grant No. FA9550-09-1-0704.

[1] Y. Aharonov and D. Bohm, Phys. Rev. **115**, 485 (1959).
[2] J. N. Winn, S. Fan, J. D. Joannopoulos, and E. P. Ippen, Phys. Rev. B **59**, 1551 (1999).
[3] P. Dong, S. F. Preble, J. T. Robinson, S. Manipatruni, and M. Lipson, Phys. Rev. Lett. **100**, 033904 (2008).
[4] Z. Yu and S. Fan, Nature Photon. **3**, 91 (2009).
[5] Z. Yu and S. Fan, IEEE J. Quantum Electron. **16**, 459 (2010).
[6] H. Lira, Z. Yu, S. Fan, and M. Lipson, arXiv:1110.5337.
[7] This normalization condition is described in detail in the Supplemental Material. It is equivalent to the normalization condition as described in Ref. [5] and is related, but not identical, to the normalization condition described in K. Busch, G. von Freymann, S. Linden, S. F. Mingaleev, L. Tkeshelashvili, and M. Wegener, Phys. Rep. **444**, 101 (2007), since here we deal with the transverse modal profiles of the waveguide.
[8] See Supplemental Material at http://link.aps.org/supplemental/10.1103/PhysRevLett.108.153901 for the derivation of this equation.
[9] W. Pauli, Rev. Mod. Phys. **13**, 203 (1941).
[10] R. E. Peierls, Z. Phys. **80**, 763 (1933).
[11] T. T. Wu and C. N. Yang, Phys. Rev. D **12**, 3845 (1975).
[12] F. Wilczek and A. Zee, Phys. Rev. Lett. **52**, 2111 (1984).
[13] M. V. Berry, Proc. R. Soc. A **392**, 45 (1984).
[14] R. L. Espinola, T. Izuhara, M. C. Tsai, R. M. Osgood, and H. Dotsch, Opt. Lett. **29**, 941 (2004).
[15] M. Levy, J. Opt. Soc. Am. B **22**, 254 (2005).
[16] T. T. Zaman, X. Guo, and R. J. Ram, Appl. Phys. Lett. **90**, 023514 (2007).
[17] N. Kono, K. Kakihara, K. Saitoh, and M. Koshiba, Opt. Express **15**, 7737 (2007).
[18] M. C. Tien, T. Mizumoto, P. Pintus, H. Kroemer, and J. E. Bowers, Opt. Express **19**, 11 740 (2011).
[19] M. S. Kang, A. Butsch, and P. St. J. Russell, Nature Photon. **5**, 549 (2011).
[20] Z. Yu and S. Fan, Nature Photon. **5**, 517 (2011).
[21] P. Dong, S. F. Preble, J. T. Robinson, S. Manipatruni, and M. Lipson, Phys. Rev. Lett. **100**, 033904 (2008).
[22] S. F. Preble, Q. Xu, and M. Lipson, Nature Photon. **1**, 293 (2007).
[23] R. Soref and B. Bennett, IEEE J. Quantum Electron. **23**, 123 (1987).